Optical transitions in GaAs:Fe studied by Fourier-transform infrared spectroscopy

K. Pressel, G. Rückert, and A. Dörnen

4. Physikalisches Institut, Universität Stuttgart, D-7000 Stuttgart 80, Germany

K. Thonke

Abteilung Halbleiterphysik, Universität Ulm, D-7900 Ulm, Germany

A high-sensitivity Fourier-transform emission and absorption technique has been used to study the iron-related optical transitions in GaAs. Improved photoluminescence and absorption spectra between 2500 and 3500 cm^{-1} allow a detailed analysis of the four routinely observed zero-phonon lines corresponding to the $^5T_2 \rightarrow {}^5E$ internal transitions within the ^5D ground state of Fe^{2+} in tetrahedral environment, and of the corresponding phonon and vibrational sidebands. We derived a rather complete level scheme of the ^5D sublevels at Fe^{2+} in GaAs from the transition energies found in absorption spectra recorded at higher sample temperatures in the energy range between 2900 and 3400 cm^{-1}. Some of the excited states were found to be significantly lowered by dynamical Jahn-Teller contributions. The iron-related line labeled 1a, which has now also been observed in absorption, is tentatively ascribed to a Fe^{3+} transition $^4T_1 \rightarrow {}^6A_1$.

I. INTRODUCTION

GaAs is the most frequently studied III-V semiconductor because of its importance for applications in high-speed electronic circuits. III-V alloys are often contaminated by 3d elements which act as deep traps. Iron, in particular, is such a contamination that can introduce shunt paths. In GaAs, as in InP, the existence of the Fe^{2+} state is verified by optical measurements, and the neutral Fe^{3+} state is identified by ESR. An overview of spectroscopy summarizing optical, ESR, and transport measurements on Fe-doped InP, GaAs, and GaP was recently presented by Bishop.[1] The internal ^5D transitions at Fe in GaAs have been detected in absorption[2,3] and later also in photoluminescence (PL).[4-6] In recent PL studies, Leyral, Charreux, and Guillot[7] made use of the fact that the Fe^{2+} PL signal is efficiently pumped when the sample is excited below the band gap.[6] Whereas in previous work only spectra with limited resolution were reported, we present here a detailed study of the $^5T_2 \rightarrow {}^5E$ internal transitions and the corresponding phonon and vibrational sidebands in high resolution. Fourier-transform-infrared (FTIR) spectroscopy increases the sensitivity in the midinfrared region by about two orders of magnitude for both absorption and luminescence, as compared to conventional monochromator techniques used before. In our measurements the light was analyzed by a BOMEM DA3.01 FTIR spectrometer, which offers a maximum unapodized resolution of 0.01 cm^{-1}. In PL measurements either a krypton-ion laser (647 nm) or a tunable Ti:sapphire laser (1.1–0.87 μm) was used for excitation. The PL and absorption spectra between 2000 cm^{-1} and 3500 cm^{-1} were detected by a liquid-nitrogen-cooled InSb detector. The GaAs samples were either polycrystalline CZ-grown samples doped in the melt or semi-insulating GaAs single crystals diffused by Fe at temperatures between 650 °C and 850 °C for several hours in evacuated ampoules.

II. ZERO-PHONON LINES

A tetrahedral crystal field splits the ^5D ground state of the Fe^{2+} free ion into a lower-lying ^5E level and a $^5T_2$ excited state. This is depicted schematically in the inset of Fig. 1. Spin-orbit coupling introduces further splittings. The $^5T_2$ excited state is split into six levels, (Γ_5), (Γ_4, Γ_3), and ($\Gamma_5', \Gamma_4', \Gamma_1$) in ascending order, which group to states of approximate total-angular momentum $J' = 1$, $J' = 2$, and $J' = 3$, respectively.[8] The ^5E ground state is split, by interaction with the $^5T_2$ state, into five close, approximately equally spaced levels Γ_1, Γ_4, Γ_3, Γ_5, and Γ_2. As all states have even parity, no electric-dipole transitions are allowed within the unperturbed substates of ^5D. However, mixing of these ^5D states with higher-lying states of Fe^{2+} with odd parity, mediated by the U^3 contribution of the crystal field, makes optical transitions allowed.[9] Arrows in the level scheme indicate the four dipole-allowed PL transitions emanating from the lowest $^5T_2$ substate.

Figure 1 shows a low-temperature PL spectrum of the four zero-phonon (ZP) lines, together with the corresponding phonon sideband. The amply structured sideband shows several features that will be discussed in detail below. As already recognized earlier in less resolved spectra, the spacings of the four ZP lines are not equal[3,7] and the full widths at half maximum (FWHM) are not identical.[7] The spectroscopic data on these four ZP lines are summarized in Table I. While the two high-energy peaks have a FWHM of about 0.1 cm^{-1}, the two low-energy peaks are more than 2 cm^{-1} broad in our samples. The PL linewidths of ZP1 and ZP2 of Fe^{2+} in GaAs are more than twice as large as the linewidths of the corresponding transitions of Fe^{2+} in InP and GaP. Unlike the InP:Fe^{2+} case, the FWHM of the ZP lines in absorption is about the same as in PL in our samples.

Lines 1 and 2 are mainly Gaussian in shape at 4.2-K sample temperature. We interpret the linewidth of these
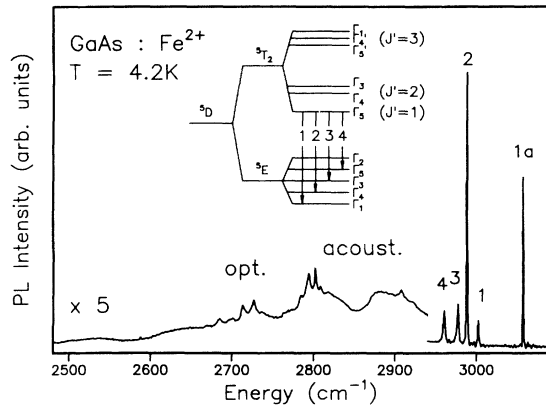
FIG. 1. Fourier-transform PL spectrum of the internal d-shell transitions at GaAs:Fe^{2+}. The sample was excited with below-band-gap light (≈ 1 μm) of a Ti:sapphire laser. Besides the four routinely observed ZP lines and their phonon replica, an additional, independent transition $1a$ is observed. The spectrum is corrected for background radiation. The inset shows a level scheme for $Fe^{2+}(^5D)$ and the four PL transitions.

lines as being determined by random microscopic strains that vary from crystal to crystal. Since lines ZP3 and ZP4 possess an essentially Lorentzian shape, we assume that these lines are lifetime broadened due to a phonon relaxation process from their final states to the lower state Γ_1 and Γ_4 of the ^5E manifold, respectively. Such a nonradiative transition to the lowest Γ_1 is forbidden for transition ZP2, ending on a Γ_4 state, since only crystal phonons of character Γ_3 can couple to the orbital part of the ^5E states and mediate such a process.

With increasing sample temperature, lines ZP1 and ZP2 broaden rapidly and change their shape from Gaussian to Lorentzian. At these higher temperatures, phonons absorbed from the thermal background can eject the electrons into close-lying excited states, thus reducing the effective lifetime of either the initial or final state of the transition. Preliminary data on the temperature dependence of the half width suggest an activation energy of this process in the range 15–30 cm^{-1}. This fits either the spacing of states within the ^5E ladder or the spacing of the two lowest substates of the $^5T_2$ manifold.

Both ZP1 and ZP2 show an isotopic fine structure, where the weaker component of ^{54}Fe is located ≈ 0.35 cm^{-1} below the dominant ^{56}Fe component, and the ^{57}Fe and ^{58}Fe are smeared out. Such fine structures introduced by the four stable Fe isotopes are observed in InP:Fe (Refs. 10 and 11) and GaP:Fe,[12] also.

The splitting of the ^5D state in a crystal field of T_d point-group symmetry can be described in good approximation by crystal-field theory. We determined the crystal-field splitting parameter Dq and the spin-orbit coupling parameter λ by solving the Hamiltonian[8]

$$H = H_{CF} + H_{s.o.} = B_4(O_4^0 + 5O_4^4) + \lambda L \cdot S \,,$$

$$L = 2 \,, \quad S = 2 \,, \quad B_4 = -Dq/12 \quad (1)$$

numerically, and fitting the theoretical values to the experimental transition energies of lines ZP1 to ZP4. The best agreement between theory and experiment was obtained with the values $Dq = 320.6$ cm^{-1} and $\lambda = -90.33$ cm^{-1} (for results see Table I). These values are slightly different from those determined in earlier work by Ippolitova and Omel'yanovskii,[3] who quoted Dq to be 299.5 ± 1 cm^{-1} and λ to be -77 ± 6 cm^{-1}. Our values are different from the latter ones since, from their less-resolved spectra Ippolitova and Omel'yanovskii made assignments of transitions to excited $^5T_2$ states totally different from ours, and partially ascribed shifts of levels to Jahn-Teller effects.

If we assume that the Dq and λ parameters derived by us are correct with the limitations discussed below, the reduction of the spin-orbit coupling parameter λ from its free-ion value $\lambda_0 = -103$ cm^{-1} is moderate, indicating that only weak covalency effects or influences of a weak dynamical Jahn-Teller effect are present. However, the absolute values of both parameters Dq and λ have to be treated with some care: The Hamiltonian (1) certainly oversimplifies the description of the Fe^{2+} system. A more elaborate theory has to take into account influences on the position of the $^5T_2$ sublevels by mixing of these levels with higher Fe^{2+} states, shifts due to covalency effects, or a dynamical Jahn-Teller (DJT) effect as considered for the system ZnS:Fe by Ham and Slack.[13] Hints to the occurrence of a DJT effect in the present GaAs:Fe system can be found in the energy position of

TABLE I. Experimental and theoretical values for the four main zero-phonon transitions 1 to 4 at Fe^{2+} (isotope ^{56}Fe) and for line $1a$, which is tentatively ascribed to Fe^{3+}. The theoretical values were calculated with values $Dq = 320.6$ cm^{-1} and $\lambda = -90.33$ cm^{-1}, which fit the energies of the four ZP transitions best. The relative values given for the PL intensities are valid for typical samples and are subject to changes by variation of excitation, temperature, and sample spot (see text).

| | | Absolute energy (cm^{-1}) | | FWHM | | Relative PL intensity | | |
| | | | | | | | | |
Line	^5E level	PL experiment 2.1–4.2 K	Theory	PL 2.1–4.2 K	Abs. 4.2 K	Ti:sapphire 2–4.2 K	16 K	Kr laser 2 K
1	Γ_1	3001.9	3001.68	0.11	0.1	33	50	42
2	Γ_4	2987.6	2988.84	0.12		100	100	100
3	Γ_3	2977.0	2975.93	2.3		21	44	29
4	Γ_5	2960.1	2960.52	2.4		19	36	24
1a		3056.8		0.23	<0.4	26	13	2

some excited $^5T_2$ states which show up in absorption (see Sec. III C). Thus we have to be aware that the $\Gamma_5(^5T_2)$ initial state of the ZP1 to ZP4 PL transitions might also be lowered significantly from its position predicted theoretically by pure crystal-field theory.

For all three systems, InP:Fe^{2+}, GaP:Fe^{2+}, and GaAs:Fe^{2+}, the theoretically calulated spacings of the four ZP lines differ in the same way from the experimental ones. When the parameters Dq and λ are determined by a least-squares fit as described above, and the theoretical line positions calculated from these parameters are compared to experiment, line ZP2 is always predicted at an excessively high energy of ≈ 0.6 cm^{-1}, and line ZP3 at an excessively low energy of ≈ 1 cm^{-1}. This systematic error must have its origin in the neglect of some additional interactions not taken into account in the crystal-field Hamiltonian Eq. (1).

When our samples were excited in the bulk by the ≈ 1-μm radiation of a Ti:sapphire laser, all our PL spectra showed an intense peak labeled "1a" in addition to the four intense ZP lines. This peak was first detected in PL by Leyral, Charreux, and Guillot.[7] The data of the additional line 1a are also summarized in Table I, but will be discussed in a separate paragraph below. When the samples are excited with the above band-gap light of a Kr$^+$-ion laser (514 nm), transition 1a almost disappears in relation to the ZP1, ZP2, ZP3, and ZP4 lines.

In our PL spectra, the ratio of the intensities of the Fe^{2+}-related ZP1–ZP4 lines and the relative intensity of line 1a varies with the sample spot excited. Keeping the laser excitation constant (below band gap) and sample temperature constant (e.g., at 4.2 K), we found spots where ZP1 vanishes completely and ZP2 is also lowered appreciably (see middle part of Fig. 2). The simplest explanation for this behavior is that a part of the emitted Fe^{2+} luminescence is reabsorbed by other Fe^{2+} ions, which are in the ground state. Since the concentration of Fe is often very inhomogeneous, especially in regions near the surface,[6] and also the Fermi level is subject to local variations, a local variation of reabsorption is expected. At low sample temperatures the higher Fe^{2+} ^5E states are populated only weakly, so besides ZP1, only ZP2 is partially affected by reabsorption processes. On all sample spots, ZP3 is approximately of equal intensity as ZP4.

On sample spots with the highest relative ZP1 intensity we determine an intensity ratio of $I_{ZP1}:I_{ZP2}:I_{ZP3}:I_{ZP4}$ $=1.7:5.2:1.1:1$ at 4.2 K sample temperature. This ratio changes slightly for higher temperatures (see lower part of Fig. 2) and approaches the theoretically predicted value of 4:9:4:3, which is derived in a perturbation approach,[13] or the theoretical ratio of 47:100:50:34 found in a complete numerical treatment with the parameters λ and Dq given above. These relative line intensities are altered further if the influence of a dynamical Jahn-Teller effect is taken into account.[14]

A less dramatic change of the ZP1–ZP4 relative intensity is observed when the excitation power is varied by a factor of 30 in the range from ≈ 3 mW to 100 mW, focused onto a spot ≈ 1 mm in diameter. ZP1 increases approximately by a factor of 4, and ZP2 is also augmented
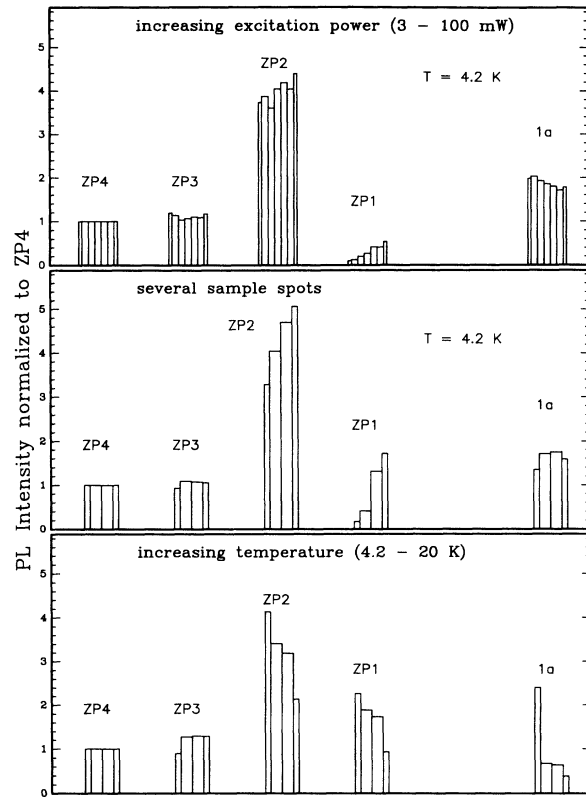
FIG. 2. Variation of the relative intensities of the Fe^{2+} lines ZP1, ZP2, ZP3, and ZP4, and line 1a upon change of several parameters. Since the lines have different FWHM, the area under the respective lines was determined either by direct integration of the spectra or by a decomposition into Lorentz-type lines in the case of overlapping lines recorded at a high sample temperature.

slightly, whereas ZP3 remains almost constant. Again, this can be understood when reabsorption is assumed, since a change of the excitation power causes a change of the quasi-Fermi level and thus alters the population of the lowest Fe^{2+} states.

The behavior of line 1a is very remarkable under these different measurement conditions. It only decreases slightly upon an increase in the excitation power and thus shows an opposite, but much weaker, dependence on excitation than the ZP1 line shows. Recording spectra on different sample spots yields dramatic changes of ZP1 (and ZP2) with an even totally vanishing ZP1 line on some specific spots, but leaves line 1a practically constant within experimental uncertainty. (This uncertainty is determined mainly by uncontrolled variations in the sample temperature.) Also, the sample temperature has a strong influence on line 1a. At temperatures around 2 K it is stronger than ZP4 but then decreases continuously, vanishing totally at around 30 K.[15] From an Arrhenius plot of the 1a PL intensity we determine a deexcitation energy of ≈ 6 cm^{-1} for the underlying luminescence process (see Sec. IV).

III. STOKES AND ANTI-STOKES
PHONON SIDEBANDS

A. Photoluminescence

The low-temperature PL spectrum of Fig. 3 shows the Fe^{2+}-related vibrational sideband in more detail. Due to much better resolution than that achieved hitherto, several features were found and unambiguous assignments can be made (Table II). Between 2650 cm^{-1} and 2950 cm^{-1} we observe coupling of the four ZP lines to multiple resonant modes leading to groups of lines with identical spacings superimposed on broader humps. The energies of these Fe-specific modes are 83 cm^{-1} (RM1), 265 cm^{-1} (RM2), and 275 cm^{-1} (RM3), respectively. These series of vibrational replicas are indicated by the sets of connected arrows in Fig. 3. These modes were resolved in part already by Leyral, Charreux, and Guillot,[7] but every peak was interpreted as a replica due to an independent phonon. The asymmetric hump with maximum at about 80 cm^{-1} below the most intense line, ZP2, can be attributed to coupling to TA phonons at the X and L points, which have energies of 79 and 64 cm^{-1}, respectively.[16] RM2 and RM3 can alternatively be ascribed to LO- and TO-phonon replicas with slightly changed phonon energy.

Between the TA and the TO-LO region another broad maximum is found at $\simeq 2800$ cm^{-1}, which can be ascribed to coupling of LA and/or two TA phonons. The sharper structures superimposed come up and disappear in proportion to line $1a$, depending on temperature, excitation, etc. At least five distinct phonon peaks can be distinguished (see Table II). The energy spacing of the uppermost three peaks is equal to the spacing of the subcomponents of line $1a$, which are visible at higher sample temperatures (see upper trace in Fig. 3 and, for a more
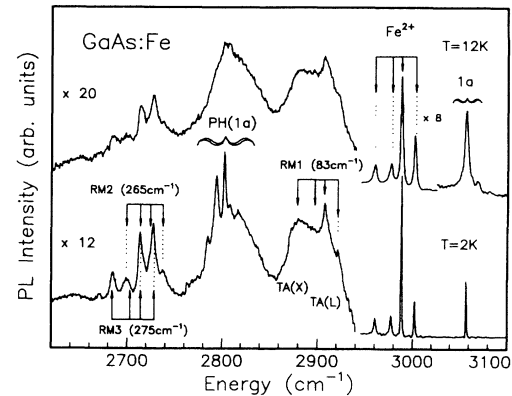
FIG. 3. FTPL spectrum of the phonon sideband, recorded at two different sample temperatures. We observe three different Fe-specific resonant modes which couple to the Fe^{2+} ZP transitions and which we label RM1–RM3. These are superimposed on broader humps introduced by coupling to conventional optical and acoustical lattice modes. Arrows indicate groups of phonon sidebands replicating the ZP lines. PH ($1a$) are replicas of the $1a$ line, as is evident from temperature-dependent measurements.

detailed discussion, Ref. 17.) The complexity of this phonon-replica spectrum indicates either that $1a$ line is emitted by a defect with symmetry lower than T_d, thus allowing for a variety of normal vibrational modes, or that this spectrum is emitted by a defect subject to a Jahn-Teller effect, causing a complicated vibronic level system. For sample temperatures above 8 K, our phonon sideband PL spectra look similar to the spectrum published by Leyral, Charreux, and Guillot which was claimed to be recorded at 4.2 K sample temperature.[7]

TABLE II. Spectral data of phonon sidebands in PL and absorption (Figs. 3 and 4). Besides coupling to undisturbed lattice modes such as TA, LA, etc., resonances due to Fe-specific resonant modes RM1 to RM3 are observed. The phonons in the lower part of the table are replicas of the $1a$ line. Their energy is given relative to the $1a$ line.

| Photoluminescence | | Absorption | |
Relative energy (cm^{-1})	Interpretation	Relative energy (cm^{-1})	Interpretation
~65	TA(L)	~65	TA(L)
~80	TA(X)	~80	TA(X)
~150	2TA	~110	TA(W)
~210	LA	~210	LA
83	RM1		
265	RM2		
275	RM3		
~270	TO	~270	TO
~295	LO	~295	LO
241			
249			
255	PH ($1a$)		
263			
272			

B. Absorption

The "anti-Stokes" phonon sideband observed in absorption measurements at 2.1 K [see Fig. 4(a)] mainly shows coupling to normal lattice modes (TA, LA, TO, LO) and combinations of these. Similar to the cases of InP:Fe^{2+},[10] and GaP:Fe^{2+},[12] only weak traces of Fe^{2+}-specific phonon replicas, which are stronger in PL, can be found in absorption. From spectra recorded with a resolution of 0.5 cm^{-1} (PL) and 0.8 cm^{-1} (absorption), we find a stronger total phonon coupling in absorption than in PL (i.e., the $^5T_2$-excited state for some reason couples

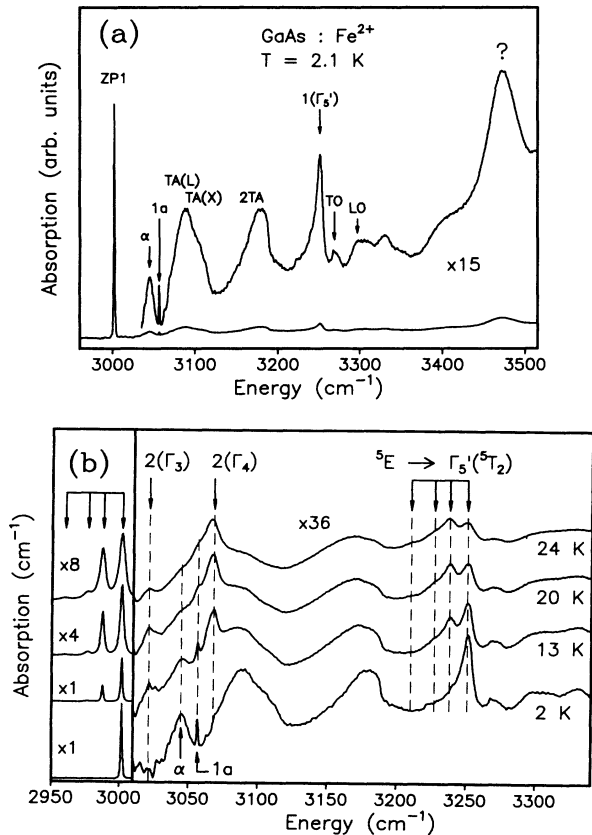FIG. 4. (a) The phonon sideband in absorption at 2.1-K sample temperature. At this low temperature, only ZP line 1 is observable. Coupling to normal lattice modes dominates, whereas the Fe-specific resonant modes only lead to weak signatures. The relatively sharp peak denoted by 1 (Γ_5') is ascribed to a transition from the lowest ^5E state Γ_1 to the excited Γ_5' state of the $^5T_2$ manifold. The origin of the broad peak at 3472 cm^{-1} (marked by ?) is currently not clear. For a discussion of 1a and α, see text. (b) The absorption sideband recorded at different sample temperatures. Upon temperature increase, several hot-line transitions starting on higher ^5E substates add to the spectrum. The group between 3200 cm^{-1} and 3250 cm^{-1} is identified with a transition to the next-higher Γ_5 state of the $^5T_2$ manifold. At 3020.6 cm^{-1} and 3066.6 cm^{-1}, transitions emerge which start on the second-lowest level, the $\Gamma_4(^5E)$ state, and which end on the Γ_3 or Γ_4 state of the $^5T_2$ manifold. The 1a and α lines are transitions not directly at Fe^{2+}, and disappear together rapidly.

more strongly to phonons than the ^5E ground state does). The respective Huang-Rhys factors are estimated at 0.8 in PL and 2 in absorption. Hence, the resonant modes could partially be hidden in the broader spectral features caused by coupling to normal lattice modes.

Among the ZP transitions, only line ZP1 is visible at low sample temperature, since only the lowest $\Gamma_1(^5E)$ state is occupied. If the sample temperature is increased [Fig. 4(b)], the higher ^5E substrates are also thermally populated, and the respective ZP transitions, in addition to their corresponding phonon replicas, emerge in the spectrum. The ZP lines obviously broaden rapidly from a FWHM of 0.5 cm^{-1} at 4.2 K to $\simeq 10$ cm^{-1} at 24 K, at the same time changing their shapes from Gaussian profiles to Lorentzian shapes. This indicates, that the effective lifetime of the electronic transitions is reduced upon a temperature increase.

Similar to the ZP lines, the phonon replicas also smear out rapidly. The origin of the intense hump at 3472 cm^{-1} also observed in the spectra of Ippolitova and Omel'yanovskii[3] remains presently unclear. Although its energy spacing from the ZP lines corresponds to the sum of a (LO+LA) combined phonon, its coupling strength contradicts this assignment. This line is Gaussian in shape, seems to build up the onset of a thresholdlike step in absorption, and is followed by onefold and twofold TA-phonon replicas.

Line 1a, hitherto reported in PL only, is also observed by us in absorption at the same energy. Another broader peak labeled α (Ref. 7) in Fig. 4(b), located 12 cm^{-1} below 1a, has a similar dependence on temperature as the latter line. Peak α has no counterpart in PL. If α was a transition belonging to 1a due to its similar temperature dependence, it should start on the same lower state, but end on a level $\simeq 12$ cm^{-1} below the 1a absorption final state. As a consequence, it should then show up in PL also, which is not the case. Thus its origin remains presently unclear.

C. Transitions to higher energy levels of the $Fe^{2+}(^5T_2)$ manifold

In the absorption phonon sideband of Fig. 4(b) several additional peaks show up which have no counterpart in PL. We assign these peaks to transitions from $Fe^{2+}(^5E)$ to excited electronic states of the Fe^{2+} upper-$^5T_2$ manifold. Symmetry arguments only allow electric-dipole transitions from the $\Gamma_1(^5E)$ ground state to Γ_5 states out of the $^5T_2$ manifold. Thus at 2.1 K, only two of the internal d-d transitions can be observed (see Fig. 5). At higher temperatures the second ground state $\Gamma_4(^5E)$ becomes thermally populated. From a Γ_4 initial state, symmetry allows electric-dipole transitions to Γ_5, Γ_4, Γ_3, and Γ_2 states. From the $\Gamma_3(^5E)$ level, which becomes populated only at even higher temperatures, transitions to Γ_5 and Γ_4 are allowed.

In the spectrum recorded at 2 K, a peak 249.5 cm^{-1} higher in energy than ZP line 1 (i.e. at $\simeq 3250$ cm^{-1}) is detected. We identify it with the transition from $\Gamma_1(^5E)$ to $\Gamma_5^9(^5T_2)$. Upon temperature increase, the corresponding transition starting on the next higher $\Gamma_4(^5E)$ level

shows up. All the observed transitions and the corresponding wavelengths are summarized in the level scheme of Fig. 5.

At still higher temperature, also an indication of the next "hot lines," the transitions from the $\Gamma_3(^5E)$ and $\Gamma_5(^5E)$ to the $\Gamma_5'(^5T_2)$ level show up. The spacing of these lines is identical to that of the 4 ZP transitions, represented in Fig. 4(b) as a set of connected arrows, which replicates the pattern of the ZP lines. The energy spacing between the excited $\Gamma_5'(^5T_2)$ and the $\Gamma_5(^5T_2)$ level is 249.5 cm^{-1}. This value is comparable to that obtained for Fe in InP and GaP, where differences of 273 cm^{-1} and 303 cm^{-1}, respectively, were determined.[11,12] The FWHM of the peak is approximately 4 cm^{-1} at low temperature, i.e., eight times larger than the FWHM of ZP lines 1 and 2. Since electrons in the excited $\Gamma_5'(^5T_2)$ state can relax fast into the lowest state Γ_5 of the $^5T_2$ manifold, via nonradiative processes, an increased half-width due to lifetime broadening is expected. Also in this respect, we found a similar behavior for the systems InP:Fe and GaP:Fe.[10,12]

Transitions to the $\Gamma_3(^5T_2)$ and $\Gamma_4(^5T_2)$ states, with positions between $\Gamma_5(^5T_2)$ and $\Gamma_5'(^5T_2)$, are found in the absorption spectrum close to lines ZP1–ZP4. Since no transitions from the lowest $\Gamma_1(^5E)$ state to Γ_3 or Γ_4 are possible, only hot lines starting on the $\Gamma_4(^5E)$ level are observable. At two energies, peaks grow in at sample temperatures around 7 K: at 3021 cm^{-1} (i.e., 33 cm^{-1} above line ZP2), and at 3069 cm^{-1} (i.e., 81 cm^{-1} above ZP2). Simple crystal-field theory would predict the Γ_3 state out of $^5T_2$ to be located $\simeq 17$ cm^{-1} above the Γ_4 state for values Dq and λ derived above, but this order can be interchanged by a dynamical Jahn-Teller effect.

FIG. 5. Level scheme for Fe^{2+} in GaAs. Crystal-field (H_{CF}) and spin-orbit (H_{LS}) interactions lead to multiple splittings. In PL, four zero-phonon transitions denoted by numbers 1–4 are observed; the energies of these are written in the arrows. In addition, several transitions to excited states of $^5T_2$ are found. The energies of these are lower than those obtained from theoretical calculations. The energy lowering is mainly ascribed to a dynamical Jahn-Teller effect, plus mixing with ligands and/or higher states (see text). Since we fitted the crystal parameters Dq and λ to the four ZP transitions, we arbitrarily kept constant the lowest level Γ_5 of $^5T_2$ in this scheme.

Ham and Slack have shown that for coupling of these states to E-type phonons with $\hbar\Omega < \lambda$ the Γ_3 state is pulled down below the Γ_4 state (see Fig. 4 in Ref. 13). From our spectra recorded on GaAs:Fe^{2+}, we cannot decide which state is lower. The next hot-line transitions, which start on the $\Gamma_3(^5E)$ level, should come in at around 25 K. They are not experimentally observable since, due to lifetime broadening, these lines are smeared out too much and, therefore, are lost in the background. Since indications exist that these states are reversed in energy in the InP:Fe^{2+} and GaP:Fe^{2+} systems,[12,18] we assume a similar effect to occur for the system under investigation here.

IV. DISCUSSION OF LINES "1a" AND "α"

As already mentioned in Sec. III A, at an energy of 3056.8 cm^{-1} a very sharp zero-phonon line "1a" shows up, which is also found in the low-temperature absorption spectra. For this line that close to the internal Fe^{2+} transitions, no analog is known in the systems InP:Fe and GaP:Fe. Whereas in PL, dependent on the sample temperature and excitation conditions, this line is higher in intensity than line ZP4 of the Fe^{2+} internal transitions, in absorption it is only about 1/100 of ZP1 at 2 K sample temperature (1/300 of ZP1 at 6 K). Line 1a disappears rapidly in the absorption spectra recorded at higher sample temperatures. It is not present in samples which are nominally free of iron, but comes up along with the Fe^{2+} transitions after diffusion of GaAs samples with iron. Leyral, Charreux, and Guillot[19] proposed a complex containing iron to be responsible for this transition.

In preliminary stress measurements on lines ZP1, ZP2, and 1a, we find line 1a to smear out and disappear rapidly in an identical manner for stress along the three crystal axes [100], [111], and [110]. Whereas the Fe^{2+} transitions ZP1 and ZP2 show a hydrostatic shift toward higher energy, the 1a line is shifted downward (along with its phonon replicas at $\simeq 2800$ cm^{-1}).

PL lifetime measurements on line 1a[15] determine a monoexponential decay of this line with a time constant of 1.9 ± 0.3 ms. Such a long time constant is typical for

FIG. 6. Tentative model for the excitation and deexcitation of Fe^{2+} in Fe^{3+} in GaAs when, in PL experiments, below-band-gap excitation is used. The levels of Fe^{3+} are drawn at an arbitrary position in the band gap.

electronic dipole-forbidden transitions. Therefore, we ascribe the $1a$ line to a Fe^{3+} $^4T_1 \rightarrow {}^6A_1$ transition. For the transition identical in nature at the isovalent defect GaP:Mn^{2+}, a time constant of 1.5 ms was measured.[21] In contrast, for the Fe^{2+} ZP lines a much shorter decay time of $\simeq 10$ μs at a 10-K sample temperature is reported.[21,15] The observation of a threefold fine structure of line $1a$ in recent PL and absorption experiments[17] also fits to the proposed $^4T_1 \rightarrow {}^6A_1$ transition, since the degeneracy of the $^4T_1$ state is lifted by a tetrahedral crystal-field and spin-orbit coupling. We consider the excited substates of $^4T_1$ (which are found 6 cm^{-1} and 13 cm^{-1}, respectively, above the $^4T_1$ lowest state) to be responsible for the decrease of the $1a$ PL intensity upon increase of sample temperature. Transitions from these excited states to the $^6A_1$ ground state are much less allowed than from the $^4T_1$ lowest state, as can be seen from absorption measurements.[17]

The observation that the ratio of $1a$ line to the Fe^{2+} transitions (more precisely, those which are not affected by reabsorption, i.e., ZP3 and ZP4) at a given sample temperature is independent of the sample spot and only weakly dependent on excitation can be understood assuming two level schemes coupled by energy transfer processes, as depicted in Fig. 6. The Fe^{2+} ^5E and $^5T_2$ states are located at $\simeq 0.8$ eV and 1.15 eV above the valence-band (VB) edge, respectively.[1] With below-gap excitation the Fe^{2+} PL can be pumped by charge-transfer transitions from Fe^{3+} to $[Fe^{2+}({}^5T_2)$, hole (VB)]. The electron excited from the VB into the $^5T_2$ state then relaxes into the ^5E ground state, emitting the ZP1, ZP2, ZP3, and ZP4 PL lines. The hole left back in the VB relaxes to the VB edge and can be bound in shallow effective-mass-like states at Fe^{2+}.[17] The complex of an electron in the ^5E state and a shallow bound hole has still an energy of $\simeq 0.8$ eV. When the hole recombines, the iron changes its charge state to Fe^{3+}. We propose that the energy of the electron-hole recombination process is partially transferred to Fe^{3+}, which is left after the recombination in its $^4T_1$ state, and the excess energy is transferred in an Auger-type process to free carriers. Finally, the recombination of the electron at Fe^{3+} emits the $1a$ line. Since in this model both PL processes, the emission of lines

ZP1, ZP2, ZP3, and ZP4 and emission of line $1a$, take place sequentially at the *same* Fe atom, the constancy of their relative intensities can easily be understood. We ascribe the strong decrease of the $1a$ PL intensity with increasing temperature to the fact, that the shallow bound hole at Fe^{2+} is thermally ejected into the valence band, thus reducing the probability of the (e, h) recombination *directly* at Fe^{2+} and, as a consequence, reducing the pumping into the excited $Fe^{3+}({}^4T_1)$ state.

With above-bandgap excitation, not only free holes but also free electrons are generated, which can recombine with the Fe^{2+} bound holes. This process again is competitive with the recombination of the $Fe^{2+}({}^5E)$ electron with shallow bound holes, and thus can explain the dramatic reduction of the $1a$ PL intensity when, in our experiments, excitation at 488 nm with an Ar^+ ion laser is applied.

An alternative model that can explain the temperature sensitivity of the $1a$ PL can be constructed, when the $Fe^{3+}({}^4T_1)$ state is assumed to be some meV below the $Fe^{2+}({}^5T_2)$ state. As a consequence, the $Fe^{3+}({}^6A_1)$ ground state must then lie also just several meV below the $Fe^{2+}({}^5E)$ state, i.e., still close to the middle of the band gap. Such a state, which corresponds to the charge transfer between Fe^{3+} and Fe^{4+}, implies the existence of a $4+$ charge state for iron in p-type samples, which has not been observed in any experiment to date.

V. CONCLUSIONS

A detailed analysis of the PL and absorption spectra allows the identification of several Fe-specific resonant phonons for GaAs:Fe^{2+}. In temperature-dependent absorption measurements, transitions to higher $^5T_2$ substates are identified. The location of the ^5D levels can be approximated well with the crystal-field model, but some characteristic differences remain. An additional transition $1a$ is tentatively ascribed to Fe^{3+} $(^4T_1 \rightarrow {}^6A_1)$.

ACKNOWLEDGMENTS

[1]S. G. Bishop, in *Deep Centers in Semiconductors*, edited by S. Pantelides (Gordon and Breach, New York, 1985), p. 541.

[2]J. M. Baranowski, J. W. Allen, and G. L. Pearson, Phys. Rev. **160**, 627 (1967).

[3]G. K. Ippolitova and E. M. Omel'yanovskii, Fiz. Tekh. Poluprovodn. **9**, 236 (1975) [Sov. Phys. Semicond. **9**, 156 (1975)].

[4]V.A. Bykovskii, V. A. Vil'kotskii, D. S. Domanevskii, and V. T. Tkachev, Fiz. Tekh. Poluprovodn. **9**, 1826 (1975) [Sov. Phys. Semicond. **9**, 1204 (1975)].

[5]W. H. Koschel, S. G. Bishop, and B. D. McCombe, in *Proceedings of the 13th International Conference on the Physics of Semiconductors*, edited by E. G. Fumi (Marves, Rome, 1977), p. 1065.

[6]P. E. R. Nordquist, P. B. Klein, S. G. Bishop, and P. G. Siebenmann, in *Gallium Arsenide and Related Compounds,*

Proceedings of the Eighth International Symposium on Gallium Arsenide and Related Compounds, edited by H. W. Thim, IOP Conf. Proc. No. 56 (Institue of Physics and Physical Society, London, 1981), p. 569.

[7]P. Leyral, C. Charreux, and G. Guillot, J. Lumin. **40 & 41**, 329 (1988).

[8]W. Low and M. Weger, Phys. Rev. **118**, 1119 (1960).

[9]G.A. Slack, F. S. Ham, and R. M. Chrenko, Phys. Rev. **152**, 376 (1966).

[10]K. Pressel, K. Thonke, and A. Dörnen, in *Proceedings of the 20th International Conference on the Physics of Semiconductors, Thessaloniki, 1990,* edited by E. M. Anastassakis and J. D. Joannopoulos (World Scientific, Singapore, 1990), p. 690.

[11]K. Pressel, K. Thonke, and A. Dörnen, Phys. Rev. B **43**, 2239 (1991).

[12]G. Rückert *et al.*, Phys. Rev. B **46**, 13 207 (1992).

[13]F. S. Ham and G.A. Slack, Phys. Rev. B **4**, 777 (1971).

[14]E. E. Vogel, O. Mualin, M. A. de Orué, and J. Rivera-Iratchet, Phys. Rev. B **44**, 1579 (1991).

[15]K. Pressel, G. Bohnert, G. Rückert, A. Dörnen, and K. Thonke, J. Appl. Phys. **71**, 5703 (1992).

[16]*Zahlenwerte und Funktionen aus Naturwissenschaften und Technik,* Londolt-Börnstein, New Series, Group III, Vol. 17, Pt. a (Springer, Berlin, 1982), p. 234.

[17]K. Pressel, G. Rückert, K. Thonke, and A. Dörnen, in *Proceedings of the 16th International Conference on Defects on Semiconductors, Bethlehem, PA, 1991,* edited by G. Davies, G. G. Deleo, and M. Stavola (Trans Tech., Zürich, 1992),
Vols. 83–87, p. 695.

[18]K. Thonke and K. Pressel, Phys. Rev. B **44**, 13 418 (1991).

[19]B. Clerjaud, in *Numerical Data and Functional Relationships in Science and Technology,* edited by O. Madelung and M. Schultz, Landolt-Börnstein, New Series, Group III, Vol. 226 (Springer, Berlin, 1989), and references therein. In a discussion about defects in GaAs, the author ascribes the '1a' line to a complex containing iron, and cites as source, P. Leyral, Institut National des Sciences Appliquées, Lyon, 1984.

[20]U. Kaufmann and J. Schneider, Adv. Electron. Electron. Phys. **58**, 81 (1982).

[21]G. Guillot, C. Benyeddou, P. Leyral, and A. Nouailhat, J. Lumin. **31&32**, 439 (1984).